

SELF CONSISTENT LOOP ANTENNA THEORY

Satish Puri

IPP 4/205

February 1982



**MAX-PLANCK-INSTITUT FÜR PLASMAPHYSIK**

**8046 GARCHING BEI MÜNCHEN**



IPP 4/205 Satish Puri Self Consistent Loop Antenna Theory

# MAX-PLANCK-INSTITUT FÜR PLASMAPHYSIK

GARCHING BEI MÜNCHEN

## SELF CONSISTENT LOOP ANTENNA THEORY

Satish Puri

IPP 4/205

February 1982

This work was performed under the terms of the agreement on cooperation between the Max-Planck-Institut für Plasmaphysik and EURATOM.

*Die nachstehende Arbeit wurde im Rahmen des Vertrages zwischen dem Max-Planck-Institut für Plasmaphysik und der Europäischen Atomgemeinschaft über die Zusammenarbeit auf dem Gebiete der Plasmaphysik durchgeführt.*

February 1982 (in English)

Abstract

An analytic theory of idealized finite loop antennas with an arbitrary current distribution is formulated. Computational steps required for the determination of the antenna current consistent with the perfectly conducting antenna surface are outlined. After dealing with the isolated antenna in free space, the effects due to the Faraday shield, the wall and the plasma are introduced. In the final form of the results, all the necessary antenna parameters may be obtained provided that the plasma surface impedance is known. The concept of the Cross-Fin Antenna which combines the twin function of wave launching and Faraday shielding in a single composite structure is introduced.

This work was performed under the terms of the agreement on association between the Max-Planck-Institut für Plasmaphysik and EURATOM.

1. INTRODUCTION

An adequate understanding of the loop antenna characteristics is desirable in view of its widespread use in the heating of thermonuclear plasmas by the ion-cyclotron (ICRF) and Alfvén waves /1-3/. Conflicting and often perplexing results of initial theoretical attempts /4-8/ indicate the need of refinement both in the models and in the analysis. The recent painstaking work of BHATNAGAR et al. /9/ has established the importance of including the effect of feeders, the three-dimensional analysis, as well as the finite antenna size. The method of solution uses a combination of induced EMF and transmission line concepts.

In this paper the loop antenna characteristics are obtained using a fully analytic solution of Maxwell's equations in-terms-of an arbitrary antenna current distribution. The current distribution, itself, however, must be determined through iterative refinement of an initial guess. Particular care is exercised in choosing a model which is analytically tractable and yet physically meaningful. Wherever possible, a physical understanding of the algebraic results is promoted.



## 2. THE IDEALIZED ANTENNA MODEL

Figure 1 is the so-called  $m = 1$  (single azimuthal variation) antenna representation in the toroidal geometry. The antenna is either "center fed" or "end fired" and may be considered as a lumped termination for the coaxial transmission line. The objectives of antenna design study may be briefly stated as

(i) The complex antenna loading  $Z^A$  presented to the transmission line. This would facilitate the design of the matching circuit to the torus chamber.

(ii) A description of the electromagnetic field " $\theta$ ", current distribution on the antenna and chamber walls, the Poynting vector into the plasma, the heating efficiency, and the antenna quality factor " $Q$ ".

(iii) An understanding of the role of the Faraday shield interspersed between the antenna and the plasma to suppress the electric field component along the major torus circumference.

For those familiar with either the self-consistent antenna problems or with the solution of wave equation in toroidal co-ordinates, the necessity of some simplification would be apparent. Following are the most important idealizations deemed necessary at this stage:

(i) The torus configuration is replaced by either the cylindrical geometry (Fig. 2) or the slab model (Fig. 3). The periodicity associated with the torus is simulated by imposing a periodicity in the z-direction with wavelength equal to an integral submultiple of the large torus-circumference. In addition, for the slab geometry, the antenna is imaged indefinitely, with a spacing one-half the minor torus circumference, in order to correctly simulate the azimuthal periodicity.

(ii) The antenna as well as the Faraday shield thickness is ignored; the co-axial transmission line is replaced by ideal, dimensionless voltage sources and the feeder holes in the wall are patched up.

(iii) The plasma is replaced by an ideal boundary of known surface impedance  $\rho_s$ .

(iv) The antenna and the wall are assumed to be perfectly conducting whereas the Faraday shield possesses an anisotropic conductivity  $\sigma_y = 0$  and  $\sigma_z = \infty$ .

(v) A final idealization consists in assuming a stream-lined current flow along the antenna length, i.e.  $J_z^A \equiv 0$ . This is perhaps, an innocuous assumption but is critical analytically as it allows one to separate the x (or y) and z-dependence of  $J^A$  and consequently of all the field quantities.



Although the idealized system, as it now stands is analytically tractable both in the cylindrical and slab geometries, the analysis of this paper is limited to the slab model. Every step in this paper, however, may be duplicated for the cylindrical coordinates.

As shown in Fig. 3, the antenna loop consists of a rectangular ribbon of length  $2l$ , breadth  $b$  and width  $2w$ , normalized by multiplying through with  $k_0 = 2\pi/\lambda_0$ , where  $\lambda_0$  is the free space wavelength. This normalization is maintained with respect to all other distance measures as well. The angular frequency and the free space impedance, too, are normalized to unity, to avoid clutter in the algebraic expressions. Exponential, spatial, as well as explicit dependences upon refractive indices are dropped, wherever, unambiguous.

### 3. ISOLATED ANTENNA IN FREE SPACE

Following the common practice in antenna theory, we first obtain the formal exact analytic solution in-terms-of an arbitrary current distribution. Subsequently, the method for determining the antenna current consistent with the assumed perfectly conducting metallic boundaries is outlined in Sec. 3.2.

### 3.1 The formal solution

It is convenient to introduce the unfolded antenna coordinate  $\xi$  with origin at  $x = y = z = 0$  and following the antenna along the loop. Let  $I_0 f_\xi(\xi) f_z(z)$  be the antenna current distribution obeying the following constraints,

$$f_\xi(\xi) = f_\xi(-\xi) \quad (3.1)$$

$$\text{and } f_\xi(0) = 1. \quad (3.2)$$

We further define the wavelength

$$\equiv \geq 4(b + 2l) \quad (3.3)$$

$$\text{and } n_{\xi 0} = 2\pi/\equiv, \quad (3.4)$$

where  $b$  and  $2l$  are the antenna breadth and length, respectively. Finally requiring that

$$f\left[\left(\equiv/2\right) + \xi\right] = -f(\xi), \quad (3.5)$$

$f(\xi)$  may be expressed as a Fourier sum

$$f_\xi(\xi) = 2 \sum_p^{+odd} F_\xi(p) \cos(n_\xi \xi), \quad (3.6)$$

where,

$$F_\xi(p) = \frac{1}{\equiv} \int_{-\equiv/2}^{\equiv/2} f_\xi(\xi) \exp(-in_\xi \xi) d\xi, \quad (3.7)$$



$$n_z = p n_{z0}, \quad (3.8)$$

and the summation extends over all odd, positive integers from 1 to  $\infty$ .

A similar Fourier decomposition of the current profile  $f_z(z)$  along  $z$  gives,

$$f_z(z) = 2 \sum_n^{+ \text{odd}} F_z(n) \cos n_z z \quad (3.9)$$

where,

$$F_z(n) = \frac{1}{\lambda_{z0}} \int_{-\lambda_{z0}/2}^{\lambda_{z0}/2} f_z(z) \exp(-in_z z) dz, \quad (3.10)$$

and,

$$n_z = n n_{z0} = 2\pi n / \lambda_{z0}, \quad (3.11)$$

is the refractive index in the z-direction and  $\lambda_{z0}$  is twice the spacing between adjacent loops.

We remind the reader that independent Fourier analysis of the antenna current has been possible due to the assumption of streamlined current flow with  $J_z \equiv 0$ . Although this assumption may break down near sharp bends on wide antennas, the error introduced is not likely to be significant.

The solution for the electromagnetic field may now be obtained from the Maxwell's equations in vacuum, subject to the boundary condition that the magnetic field component  $H_z$  has a discontinuous jump at the location of the antenna current.

We may express the total antenna field  $\theta^A$  as

$$\theta^A = \theta^{AF} + \theta^{AB} + (\theta^{AS_T} + \theta^{AS_o} + \theta^{AS_b}), \quad (3.12)$$

where  $\theta^{AF}$ ,  $\theta^{AB}$  and  $\theta^{AS}$  pertain to the contributions from the antenna front surface, the antenna back and the two antenna sides taken together, respectively. We will later see that the field arising from the antenna sides has three distinct components; corresponding to a transmission line field  $\theta^{AS_T}$  plus the contributions  $\theta^{AS_o}$  and  $\theta^{AS_b}$  from the open circuit terminations at  $x = 0$  and  $x = -b$ , respectively.



### 3.11 Contributions from Antenna Front and Back

The current distribution on the antenna front ( $x = 0$ ) and back ( $x = -b$ ) may be expressed as,

$$\begin{aligned} J_y^{AF} &= I_0 f_z(z) f_{\frac{3}{2}} \left[ |y - \kappa \lambda_{y0}| \leq l \right] \\ &= -I_0 f_z(z) f_{\frac{3}{2}} \left[ |y - (\kappa + 1/2) \lambda_{y0}| \leq l \right] \end{aligned} \quad (3.13)$$

and

$$\begin{aligned} J_y^{AB} &= I_0 f_z(z) f_{\frac{3}{2}} \left[ b + 2l - |y - \kappa \lambda_{y0}| \right] \\ &= -I_0 f_z(z) f_{\frac{3}{2}} \left[ b + 2l - |y - (\kappa + 1/2) \lambda_{y0}| \right] \end{aligned} \quad (3.14)$$

where  $\kappa$  ranges over all integral values from  $-\infty$  to  $+\infty$ .

The Fourier components  $F_z(n)$  for the  $z$ -dependence  $f_z(z)$  are already given in (3.10). Similar Fourier analysis in the  $y$ -direction gives, for  $m = \pm$  odd,

$$F_y(m) = \frac{4n_{y0}}{\pi} \sum_p^{\text{+odd}} F_{\frac{3}{2}}(p) \frac{n_y}{n_y^2 - n_{\frac{3}{2}}^2} (1 - \gamma_1) \cos n_{\frac{3}{2}} l \sin n_y l \quad (3.15)$$

and

$$B_y(m) = -\frac{4n_{y0}}{\pi} \sum_p^{\text{+odd}} F_{\frac{3}{2}}(p) \frac{n_y}{n_y^2 - n_{\frac{3}{2}}^2} (1 - \gamma_2) \cos n_{\frac{3}{2}} b \cos n_{\frac{3}{2}} l \sin n_y l \quad (3.16)$$

where,

$$n_y = m n_{y0} = 2\pi m / \lambda_{y0} \quad , \quad (3.17)$$

$\lambda_{y0}$  is twice the spacing of adjacent loops in the y-direction while

$$\gamma_1 = (n_z / n_y) \tan n_z l \cot n_y l \quad (3.18)$$

and

$$\gamma_2 = \frac{n_y \sin n_z b \sin n_z l \sin n_y l - n_z \sin n_z (b+l) \cos n_y l + \sin n_z (b+2l)}{n_y \cos n_z b \cos n_z l \sin n_y l} \quad (3.19)$$

For the elementary current excitation,  $\exp. [i(n_x x + n_y y + n_z z - t)]$ , one obtains upon applying the boundary conditions for

$\theta_{\text{tangential}}$  at  $x = 0$ ,

$$E_x^{AF} = [u(x) n_y / 2] \exp(-|n_x x|) \quad (3.20)$$

$$E_y^{AF} = [(n_y^2 - 1) / 2 n_x] \exp(-|n_x x|) \quad (3.21)$$

$$E_z^{AF} = [n_y n_z / 2 n_x] \exp(-|n_x x|) \quad (3.22)$$

$$H_x^{AF} = [n_z / 2 n_x] \exp(-|n_x x|) \quad (3.23)$$

$$H_y^{AF} = 0 \quad (3.24)$$

and

$$H_z^{AF} = \left[ -u(x)/2 \right] \exp(-|n_x x|), \quad (3.25)$$

where  $u(\mu)$  is the discontinuity function defined by,

$$u(\mu) = \pm 1 \quad \text{for} \quad \mu \geq 0. \quad (3.26)$$

Combining (3.20) - (3.25) with (3.15) and (3.16), then multiplying (as well as summing) through  $F_z(n)$  finally gives the field contributions,  $\theta^{AF}$  and  $\theta^{AB}$  from the antenna front and back, respectively.

One must take care to replace  $x$  by  $(x + b)$  in (3.20) - (3.25) when calculating  $\theta^{AB}$ .

### 3.12 Contributions from the Antenna Sides

The antenna current in this case lies in constant  $x$ - $z$  planes and has the form

$$J_x^{AS} = I_0 f_z(z) f_x(l-x) [h(x+b) - h(x)] \sum_{k=0}^{\infty} (-1)^{k+1} \left[ \delta \left\{ \gamma - k(\lambda_{y_0}/2) - l \right\} - \delta \left\{ \gamma - k(\lambda_{y_0}/2) + l \right\} \right], \quad (3.27)$$

where  $\delta(\mu)$  is the Dirac delta function defined by the Fourier decomposition

$$\delta(\mu) = \frac{1}{2\pi} \int_{-\infty}^{\infty} \exp(i n_{\mu} \mu) dn_{\mu}, \quad (3.28)$$

and  $h(\mu)$  is the Heavyside function defined as

$$\begin{aligned} h(\mu) &= 0, \quad \text{for } \mu < 0 \\ &= 1, \quad \text{for } \mu \geq 0. \end{aligned} \quad (3.29)$$

Writing  $J^{AS}$  as the convolution product

$$\begin{aligned} J_x^{AS} &= I_0 f_z(z) \sum_{\kappa=0}^{\infty} (-1)^{\kappa+1} \left[ \delta\{\gamma - \kappa(\lambda_{\gamma_0}/2) - l\} \right. \\ &\quad \left. - \delta\{\gamma - \kappa(\lambda_{\gamma_0}/2) + l\} \right] \int_x^{x+b} \delta(x_1) f_{\xi}(l-x+x_1) dx_1, \end{aligned} \quad (3.30)$$

one is in the position to exploit the Green's function formalism. The method of solution would consist in first determining the electromagnetic fields due to the current

$$\begin{aligned} J_x^G &= I_0 \delta(x) F_z(n) \sum_{\kappa=0}^{\infty} (-1)^{\kappa+1} \\ &\quad \left[ \delta\{\gamma - \kappa(\lambda_{\gamma_0}/2) - l\} - \delta\{\gamma - \kappa(\lambda_{\gamma_0}/2) + l\} \right], \end{aligned} \quad (3.31)$$

and then obtaining the required results through convolution with  $f_{\xi}(l-x)$  and summing over  $F_z(n)$ .



As in Sec. 3.11, the field components for the elementary excitation  $\exp [i(n_x x + n_y y + n_z z)]$  are given as

$$E_x^{AS} = -i [(1-n_x^2)/n_y] g(n_y) \sin n_y y, \quad (3.32)$$

$$E_y^{AS} = u(l-y) n_x g(n_y) \cos n_y y, \quad (3.33)$$

$$E_z^{AS} = i (n_x n_z / n_y) g(n_y) \sin n_y y \quad (3.34)$$

$$H_x^{AS} = 0, \quad (3.25)$$

$$H_y^{AS} = -i (n_z / n_y) g(n_y) \sin n_y y, \quad (3.26)$$

and

$$H_z^{AS} = u(l-y) g(n_y) \cos n_y y, \quad (3.37)$$

where

$$g(n_y) = \frac{\cos [n_y \{(\lambda_{y0}/4) - l\}]}{\cos [n_y (\lambda_{y0}/4)]} \quad (3.38)$$

where

The Green's function for the impulse excitation  $\delta(x)$  can now be obtained by integrating (3.32) - (3.37), one at a time over the Fourier spectrum of the form given by (3.28). The integrand consists of the sum of residues corresponding to the singularities of  $g(n_y)$  which possesses simple poles at

$$n_y (\lambda_{y_0}/4) = m\pi/2, \text{ for } m = \pm \text{odd}. \quad (3.39)$$

The path of integration extends over the real  $n_x$  axis from  $-\infty$  to  $+\infty$  and closes back over a semicircle of radius  $R$  — in the upper or the lower half planes, respectively, for  $x \gtrless 0$ . The Green's functions  $G[\theta^{AS}]$ , obtained in the above manner are given by

$$G[E_x^{AS}] = -i K_1 \sum_m^{+\text{odd}} [(1-n_x^2)/|n_x|] \sin n_y z \sin n_y y, \quad (3.40)$$

$$G[E_y^{AS}] = i u(x) u(z-y) K_1 \sum_m^{+\text{odd}} n_y \sin n_y z \cos n_y y, \quad (3.41)$$

$$G[E_z^{AS}] = -u(x) K_1 \sum_m^{+\text{odd}} n_z \sin n_y z \sin n_y y, \quad (3.42)$$

$$G[H_y^{AS}] = -i K_1 \sum_m^{+\text{odd}} (n_z / |n_x|) \sin n_y z \sin n_y y, \quad (3.43)$$

$$G[H_z^{AS}] = u(z-y) K_1 \sum_m^{+\text{odd}} (n_y / |n_x|) \sin n_y z \cos n_y y, \quad (3.44)$$

where

$$K_1 = (2 n_{y_0} / \pi) F_z(n) I_0. \quad (3.45)$$

The final results obtained by convolving (3.40) - (3.44) in the manner of (3.30) and after summing over  $F_z(n)$  are given in the following section.

### 3.13 The total Antenna Field

Upon adding the field contributions  $\theta^{AF}$ ,  $\theta^{AB}$  and  $\theta^{AS}$  one obtains the composite antenna fields

$$\begin{aligned}
 E_x^A &= iK_2 \sum_{m \substack{+ \text{ odd} \\ m}} \sum_n \sum_p q_1 \sin n_y y \cos n_z z \\
 &\left[ u(x) \left\{ \Gamma_1 (1 - r_x^E) (1 - \gamma_1) - \Gamma_2 (1 - \gamma_3) \right\} E(x) \right. \\
 &\left. - u(x+b) \left\{ \Gamma_1 (1 - r_x^E) (1 - \gamma_2) - \Gamma_2 (1 - \gamma_4) \right\} \cos n_z b E(x+b) \right] \\
 &+ 8iI_0 \sum_n \sum_p \substack{+ \text{ odd} \\ n \quad p} F_z(n) F_z(p) \cos n_z (z-x) \square(x, b) [\delta(\gamma-1) - \delta(\gamma+1)] \cos n_z z
 \end{aligned}$$

(3.46)

$$E_y^A = -i K_2 \sum_{m,n,p}^{+ \text{ odd}} \frac{|n_x| n_y}{n_y^2 + n_z^2} q_1 \cos n_y y \cos n_z z$$

$$\left[ \left\{ \Gamma_1 (1 - r_y^E) (1 - \gamma_1) - u(l-y) \Gamma_2 (1 - \gamma_3) \right\} \xi(x) \right.$$

$$\left. - \left\{ \Gamma_1 (1 - r_y^E) (1 - \gamma_2) - u(l-y) \Gamma_2 (1 - \gamma_4) \right\} \cos n_z b \xi(x+b) \right]$$

$$- 2i u(l-y) K_2 \sum_{m,n,p}^{+ \text{ odd}} \frac{n_y}{n_y^2 + n_z^2} q_1 \frac{\sin n_z (l-x)}{\cos n_z l} \Gamma_2 \square(x,b) \cos n_y y \cos n_z z$$

(3.47)

$$E_z^A = -i K_2 \sum_{m,n,p}^{+ \text{ odd}} \frac{|n_x| n_z}{n_y^2 + n_z^2} q_1 \sin n_y y \sin n_z z$$

$$\left[ \left\{ \Gamma_1 (1 - r_z^E) (1 - \gamma_1) - \Gamma_2 (1 - \gamma_3) \right\} \xi(x) \right.$$

$$\left. - \left\{ \Gamma_1 (1 - r_z^E) (1 - \gamma_2) - \Gamma_2 (1 - \gamma_4) \right\} \cos n_z b \xi(x+b) \right]$$

$$+ 2i K_2 \sum_{m,n,p}^{+ \text{ odd}} \frac{n_z}{n_y^2 + n_z^2} q_1 \frac{\sin n_z (l-x)}{\cos n_z l} \Gamma_2 \square(x,b) \sin n_y y \sin n_z z$$

(3.48)



$$H_x^A = K_2 \sum_{m \text{ odd}} \sum_{n \text{ odd}} \sum_{p \text{ odd}} \frac{n_y n_z}{|n_x| (n_y^2 - 1)} q_1 \cos n_y y \sin n_z z$$

$$\Gamma_1 \left[ (1 - \gamma_1) \xi(x) - (1 - \gamma_2) \cos n_3 b \xi(x+b) \right] \quad (3.49)$$

$$H_y^A = K_2 \sum_{m \text{ odd}} \sum_{n \text{ odd}} \sum_{p \text{ odd}} n_z q_1 \sin n_y y \sin n_z z$$

$$\Gamma_2 \left[ u(x) (1 - \gamma_3) \xi(x) - u(x+b) (1 - \gamma_4) \cos n_3 b \xi(x+b) \right]$$

$$-8 I_0 \sum_n \sum_p \sum_{\text{odd}} q_1 \frac{\cos n_3 (l-x)}{\cos n_3 l} \Gamma_2 \square(x, b) [\delta(\gamma-1) - \delta(\gamma+1)] \cos n_z z$$

(3.50)

$$H_z^A = -K_2 \sum_{m,n,p}^{+ \text{ odd}} \frac{n_y}{n_y^2 + n_z^2} q_1 \cos n_y y \cos n_z z$$

$$\left[ u(x) \left\{ \Gamma_1 (1 - r_2^H) (1 - \gamma_1) - u(l-y) \Gamma_2 (1 - \gamma_3) \right\} \xi(x) \right]$$

$$- u(x+b) \left\{ \Gamma_1 (1 - r_2^H) (1 - \gamma_2) - u(l-y) \Gamma_2 (1 - \gamma_4) \right\} \cos n_3 b \xi(x+b) \right]$$

$$- u(l-y) 2K_2 \sum_{m,n,p}^{+ \text{ odd}} \frac{n_y}{n_y^2 + n_z^2} q_1 \frac{\cos n_3 (l-x)}{\cos n_3 l} \Gamma_2 \square(x, b) \cos n_y y \cos n_z z$$

(3.51)

where,

$$K_2 = 8 n_{y0} I_0 / \pi \quad (3.52)$$

$$q_1 = F_2(n) F_3(p) \cos n_3 l \sin n_y l \quad (3.53)$$

$$\gamma_3 = u(x) (n_3 / |n_x|) \tan n_3 l \quad (3.54)$$

$$\gamma_4 = \frac{|n_x| \sin n_3 b \sin n_3 l + u(x+b) n_3 \sin n_3 (b+l)}{|n_x| \cos n_3 b \cos n_3 l} \quad (3.55)$$

$$\Gamma_1 = (n_y^2 - 1) / (n_y^2 - n_z^2) , \quad (3.56)$$

$$\Gamma_2 = (n_x^2 - 1) / (n_x^2 - n_z^2) , \quad (3.57)$$

$$\gamma_x^E = -1 / (n_y^2 - 1) , \quad (3.58)$$

$$\gamma_y^E = -1 / n_x^2 , \quad (3.59)$$

$$\gamma_z^E = (n_y^2 - n_x^2) / [n_x^2 (n_y^2 - 1)] , \quad (3.60)$$

$$\gamma_z^H = -(n_z^2 + 1) / (n_y^2 - 1) , \quad (3.61)$$

$$\square(x, b) = [h(x+b) - h(x)] , \quad (3.62)$$

and

$$\xi(\mu) = \exp(-|n_x| \mu) . \quad (3.63)$$

The reader would recognize the five distinct sets of contributions mentioned in (3.12) which appear in (3.46) - (3.51) in the form

$$\theta^A = (\theta^{AF} - \theta^{AS_0}) \xi(x) + (\theta^{AB} - \theta^{AS_b}) \xi(x+b) + \theta^{AS_T} \quad (3.64)$$

Following are some observations regarding  $\theta^A$ :

(i) The field components  $\theta^{AF}$  and  $\theta^{AS_0}$  as well as  $\theta^{AB}$  and  $\theta^{AS_b}$  tend to cancel in pairs leaving a net contribution which is of order  $|n|^{-2}$  compared to the individual contributions.

(ii) The electric field component  $E_z$  is inherently present for  $n_y \neq 0$ . This is similar in origin to the case of  $E_z$  associated with a simple plane wave for finite  $n_y$ .

(iii) The current in the antenna sides gives rise to discontinuities in  $E_y^S$  and  $H_z^S$  in (3.47) and (3.51). Thus  $E_y^S$  and  $H_z^S$  must be separately determined in Regions I and II (see Fig. 3) and must be carefully extended beyond these regions with proper regard to symmetry and periodicity along  $y$ .

### 3.14 Voltage and Impedance

The antenna voltage may be determined from the Maxwell's equations in one of the following ways:

$$V(z) = 2 \int_0^{b+2l} E_z d\zeta \quad (3.65a)$$

$$= i \int_{-b}^0 dx \int_{-l}^l dy H_z(x, y, z) \quad (3.65b)$$



We are pleased to report that either procedure gives the result

$$\begin{aligned}
 V(z) = & 2iK_2 \sum_{mnp}^{+odd} \frac{1 - \xi(b)}{|n_x| (n_y^2 + n_z^2)} q_{v_1} \sin n_y z \cos n_z z \\
 & \left[ \left\{ \Gamma_1 (1 - \gamma_2^H) (1 - \gamma_1) - \Gamma_2 (1 - \gamma_3^-) \right\} \right. \\
 & \left. \left\{ \Gamma_1 (1 - \gamma_2^H) (1 - \gamma_2) - \Gamma_2 (1 - \gamma_4^-) \right\} \cos n_3 b \right] \\
 & + 4iK_2 \sum_{mnp}^{+odd} \frac{\Gamma_2}{n_y^2 + n_z^2} \frac{q_{v_1}}{n_3} \frac{\sin n_3 (b+l) - \sin n_3 l}{\cos n_3 l} \sin n_y z \cos n_z z
 \end{aligned}
 \tag{3.66}$$

where the superscripts over  $\gamma_3$  and  $\gamma_4$  correspond to the signs of the discontinuity functions  $u(x)$  and  $u(x + b)$ , respectively, following the  $x$  integrations.

The antenna impedances for the "center fed" and the "end fired" cases; respectively are given by

$$Z_{CF}^A = V(0) / [I_0 f_3 (b + 2l)] \tag{3.67a}$$

and

$$Z_{EF}^A = V(0) / [I_0 f_3 (b + l)] . \tag{3.67b}$$

Replacing  $V(z)$  by  $V(0)$  is possible because for the conducting antenna the voltage is independent of  $z$  for  $|z| \leq w$ .

### 3.2 Determination of Self-Consistent Current

For the conducting antenna, the electric field vanishes over the entire metallic surface except at the voltage gaps. Depending upon the location of these gaps, the antenna boundary conditions become

$$\int_0^w dz \left[ \int_0^l \left\{ |E_y(0, y, z)| + |E_z(0, y, z)| \right\} dy + \int_v^l \left\{ |E_y(-b, y, z)| + |E_z(-b, y, z)| \right\} dy + \int_0^{-b} \left\{ |E_x(x, l, z)| + |E_z(x, l, z)| \right\} dx \right] = 0 \quad (3.68a)$$

or

$$\int_0^w dz \left[ \int_0^l \left\{ |E_y(0, y, z)| + |E_y(-b, y, z)| + |E_z(0, y, z)| + |E_z(-b, y, z)| \right\} dy + \int_0^{v-b} \left\{ |E_x(x, l, z)| + |E_z(x, l, z)| \right\} dx \right] = 0 \quad (3.68b)$$

for the "center-fed" and the end fired cases, respectively.

In the numerical procedure, one is obliged to set an upper limit  $m_{\max}$ ,  $n_{\max}$  and  $p_{\max}$  on  $m$ ,  $n$  and  $p$ , respectively. Practical experience to date suggests that  $m_{\max}$ ,  $n_{\max} = (wn_{z0})^{-1}$  and  $p_{\max} = 5$  may be satisfactory choices.

As an initial guess for  $F_{\xi}(p)$  and  $F_z(n)$ , one may assume

$$f_{\xi}^0(\xi) = \cos \xi, \quad (3.69)$$

and

$$f_z^0(z) = (2w)^{-1} \text{ for } |z - \kappa(\lambda_{z0}/2)| \leq w, \quad (3.70)$$

for all integral  $\kappa$  values from  $-\infty$  to  $+\infty$ . Upon Fourier transformation (3.69) and (3.70) give, for  $p = \pm 1, \pm 3 \dots \pm p_{\max}$

$$F_{\xi}^0(p) = \frac{2n_{z0}}{\pi} \cos \frac{\pi}{2n_{z0}} (-1)^{\frac{p-1}{2}} \frac{n_z}{n_z^2 - 1}, \quad (3.71)$$

where the superscript "o" denotes initial guess.

Note that the form (3.69) chosen for  $f_{\xi}^0(\xi)$  implies that the current flow along the antenna has the free-space wave length variation. Experience in antenna theory shows that even for complex geometric configurations, the self-consistent current departs but slightly from this distribution /10, 11/. Nevertheless, these departures

may cause significant changes in the field configuration, coupling, and heating efficiency.

The computer program involves the minimization of the functionals (3.68) of the  $(n_{\max} + p_{\max} - 2)$  variables  $F_{\xi}(p)$  and  $F_z(n)$ .

One possible computational approach consists in determining  $f_z(z)$  for  $|z| \leq w$  so as to render  $V(z)$  in (3.65) constant over the antenna width. The Fourier transformation indicated in (3.10) then gives  $F_z(n)$ , which are then held fixed while computing  $F_{\xi}(p)$  using (3.68).

The result of a sample computation using the procedure outlined in this section is shown in Fig. 4. The self-consistent current for the isolated antenna system with the parameters  $b = 1/32$ ,  $2l = 3/32$ ,  $2v = 1/128$ ,  $2w = 1/16$ ,  $n_{y_0} = n_{z_0} = 2$ , and  $n_{\xi_0} = 1$  is given by

$$f_{\xi}(\xi) = 1.138 \cos \xi - 0.150 \cos 3\xi + 0.012 \cos 5\xi, \quad (3.72)$$

for  $m_{\max} = n_{\max} = 21$  and  $p_{\max} = 5$ . The self-consistent current also shows slight peaking (0.2%) at the edges along the antenna width.



Similar computations that include the full boundary value solution for the ion-cyclotron and Alfvén wave heating are now being pursued.

#### 4. BOUNDARY VALUE SOLUTION

For the case of boundaries that are uniform in the  $y$  and  $z$  directions, the effect of the boundary may be duplicated by replacing it by a surface current distribution  $J_s$  in such a manner that the total electromagnetic field  $\theta^J$  due to all  $J_s$  plus the antenna field  $\theta^A$  satisfy the prescribed boundary conditions. The problem is made much easier by following this procedure for each Fourier component  $(n_y, n_z)$  and then summing over all harmonics to obtain the composite response.

The first step for realizing this objective is to recast (3.47) and (3.51) as proper Fourier series without the discontinuity function. One obtains

$$E_y^A = -iK_2 \sum_{mnp}^{+odd} \frac{n_x n_y}{n_y^2 + n_z^2} q_1 \Gamma_1 \cos n_y y \cos n_z z$$

$$\left[ (1 - r_y^E) \left\{ (1 - r_1) \xi(x) - (1 - r_2) \cos n_3 b \xi(x+b) \right\} \right]$$

$$-iK_3 \sum_{m'n'p}^{+odd} \frac{n_x n_y'}{n_y'^2 + n_z^2} q_2 \Gamma_2 \cos n_z z$$

$$\left[ (1 - r_3) \xi(x) - (1 - r_4) \cos n_3 b \xi(x+b) \right]$$

$$-2iK_3 \sum_{m'n'p}^{+odd} q_2 \Gamma_2 \frac{n_y'}{n_y'^2 + n_z^2} \frac{\sin n_3 (l-x)}{\cos n_3 l} \square(x, b) \cos n_z z$$

(4.1)

and,

$$H_z^A = -K_2 \sum_{mnp}^{+odd} \frac{n_y}{n_y^2 + n_z^2} \Gamma_1 q_2 \cos n_y y \cos n_z z$$

$$\left[ (1 - r_z^H) \left\{ u(x) (1 - r_1) \xi(x) - u(x+b) (1 - r_2) \cos n_3 b \xi(x+b) \right\} \right]$$

$$-K_3 \sum_{m'n'p} \frac{n_y'}{n_y'^2 + n_z^2} q_2 \Gamma_2 \cos n_z z$$

$$\left[ (1 - r_3) \xi(x) - (1 - r_4) \cos n_3 b \xi(x+b) \right]$$

$$-2K_3 \sum_{3m'n'p}^{+odd} \frac{n_y'}{n_y'^2 + n_z^2} q_2 \Gamma_2 \frac{\cos n_3 (l-x)}{\cos n_3 l} \square(x, b) \cos n_z z$$

(4.2)

where

$$K_3 = (\epsilon n_{y0} / \pi) K_2 \quad (4.3)$$

and

$$q_2 = F_2(n) F_3(p) \cos n_y z \sin n_y' z \frac{n_y' \sin n_y' l \cos n_y z - n_y \sin n_y z \cos n_y' l}{n_y^2 - n_y'^2} \quad (4.4)$$

Next we express each Fourier component  $\theta(n_y, n_z)$  as

$$\theta(n_y, n_z) = \hat{\theta}(n_y, n_z) X(\xi) \exp [i(n_y y + n_z z)] \quad (4.5)$$

where  $\hat{\theta}$  is the amplitude and  $X(\xi)$  contains the exponential dependence on  $x$ . The superscripts A, F, W and P stand for the antenna, the Faraday shield, the wall and the plasma, respectively.

Before attempting to tackle the complete boundary value problem, it is instructive to study the effect of the Faraday shield on the antenna behavior.

#### 4.1 Faraday Shielding and the Cross-Fin Antenna

We limit this discussion to the electromagnetic behavior of the Faraday shield without comment on its function as a

particle screen. The field components produced by the induced current  $J_z^F$  ( $n_y, n_z$ ) in the Faraday shield are

$$E_x^F = u(x-f) (n_z/2) J_z^F \xi(x-f), \quad (4.6)$$

$$E_y^F = (n_y n_z / 2 n_x) J_z^F \xi(x-f), \quad (4.7)$$

$$E_z^F = [(n_z^2 - 1) / 2 n_x] J_z^F \xi(x-f), \quad (4.8)$$

$$H_x^F = -(n_y / 2 n_x) J_z^F \xi(x-f), \quad (4.9)$$

$$H_y^F = [u(x-f) / 2] J_z^F \xi(x-f), \quad (4.10)$$

and,

$$H_z^F = 0. \quad (4.11)$$

Applying the boundary condition  $E_z(x=f) = 0$ , gives

$$[(n_z^2 - 1) / 2 n_x] J_z^F + E_z^A(f) = 0, \quad (4.12)$$

which determines  $J_z^F(n_y, n_z)$ . For  $x \geq f$ , we obtain from (4.8) and (4.12)

$$E_z(x) = -E_z^A(f) \xi(x-f) + E_z^A(x) \equiv 0, \quad (4.13)$$

which answers the basic function expected of the Faraday shield. For  $0 \leq x \leq f$ , one obtains for  $E_x$  and  $E_z$ ,

$$E_x(x) = -(n_z/2) J_z^F \xi(x-f) + E_x^A(x) \\ = \hat{E}_z^{A_0} [1 + \{n_x n_z / (n_z^2 - 1)\} \xi\{2(f-x)\}] \xi(x) \\ + \text{terms involving } \xi(x+b)$$

$$\sim O(\hat{E}_y^{A_0}),$$

(4.14)

and,

$$E_z(x) = [(n_z^2 - 1) / 2n_x] J_z^F \xi(x-f) + E_z^A(x) \\ = \hat{E}_z^{A_0} [1 - \xi\{2(f-x)\}] \xi(x)$$

$$+ \text{terms involving } \xi(x+b)$$

$$\sim O(2n_x f \hat{E}_z^{A_0})$$

(4.15)

$$\sim O(2n_x f \hat{E}_y^{A_0}),$$

where

$$E^{A_0} = E^{AF} + E^{AS_0}, \quad (4.16)$$

is the antenna field with the exponential behavior  $E(x)$  and dominates in the region  $x \geq 0$ .

From (4.14) and (4.15) observe that there exist  $E_x$  and  $E_z$  fields in the space between the antenna and the Faraday shield. These fields may be comparable in magnitude to the  $\hat{E}_y^{A_0}$  field component responsible for coupling the fast wave into the plasma. These fields, however, disappear for  $f \rightarrow 0$ , i.e. when the Faraday shield position coincides with the antenna front surface. The corresponding practical configuration of such an antenna is shown in Fig. 5. The Faraday shield forms an integral part of the antenna in the guise of fin like rods placed across the antenna at regular intervals. The length and distribution of the fins would be determined through practical experience. The overall appearance of such an antenna-Faraday shield combination suggests the name Cross-Fin Antenna.

#### 4.2 The Complete Solution

Let  $J_y^W(x = -c)$ ,  $J_z^W(x = -c)$ ,  $J_z^F(x = f)$ ,  $J_y^P(x = a)$ , and  $J_z^P(x = a)$  be the surface currents associated with the walls, the Faraday shield and the plasma boundaries, respectively.

The boundary conditions to be satisfied are  $E_y, E_z = 0$  at  $x = -c$ ;  $E_z = 0$  at  $x = f$ ;  $E_y/H_z = \rho_f$  and  $-E_z/H_y = \rho_s$  at  $x = a$ , where  $\rho_f$  and  $\rho_s$  are the plasma surface impedances and are assumed to be known for each spectrum component  $(n_y, n_z)$ .

Solving for  $J$  gives

$$[J] = [\Psi_1] [M_1]^{-1}, \quad (4.17)$$

where

$$[J] = [J_y^W \quad J_z^W \quad J_z^F \quad J_y^P \quad J_z^P], \quad (4.18)$$

$$[M_1] = \quad (4.19)$$

$\alpha_1$	$\alpha_2$	$\alpha_2 \xi(c+f)$	$(\alpha_1 + \rho_f/2) \xi(a+c)$	$\alpha_2 \xi(a+c)$
$\alpha_2$	$\alpha_3$	$\alpha_3 \xi(c+f)$	$\alpha_2 \xi(a+c)$	$(\alpha_3 + \rho_s/2) \xi(a+c)$
$\alpha_2 \xi(c+f)$	$\alpha_3 \xi(c+f)$	$\alpha_3$	$\alpha_2 \xi(a-f)$	$\alpha_3 \xi(a-f)$
$\alpha_1 \xi(a+c)$	$\alpha_2 \xi(a+c)$	$\alpha_2 \xi(a-f)$	$(\alpha_1 - \rho_f/2)$	$\alpha_2$
$\alpha_2 \xi(a+c)$	$\alpha_3 \xi(a+c)$	$\alpha_3 \xi(a-f)$	$\alpha_2$	$(\alpha_3 - \rho_s/2)$



$$[\psi_1] = \begin{bmatrix} -E_y^A(-c) & -E_z^A(-c) & -E_z^A(f) & -E_y^A(a) + \beta_f H_z(a) & -E_z^A(a) - \beta_s H_y(a) \end{bmatrix} \quad (4.20)$$

$$\alpha_1 = -i (n_y^2 - 1) / 2 |n_x| , \quad (4.21)$$

$$\alpha_2 = -i n_y n_z / 2 |n_x| , \quad (4.22)$$

and

$$\alpha_3 = -i (n_z^2 - 1) / 2 |n_x| . \quad (4.23)$$

Knowing [J], it is a straightforward exercise to determine the composite fields in the form

$$[\theta] = \sum_m \sum_n^{\text{odd}} \exp[i(n_y y + n_z z)] \{ [\hat{\theta}^A] + [\psi_2] [M_2] \} , \quad (4.24)$$

where,

$$[\theta] = [ E_x \quad E_y \quad E_z \quad H_x \quad H_y \quad H_z ] , \quad (4.25)$$

$$[\hat{\theta}^A] = [ \hat{E}_x^A \quad \hat{E}_y^A \quad \hat{E}_z^A \quad \hat{H}_x^A \quad \hat{H}_y^A \quad \hat{H}_z^A ] , \quad (4.26)$$

$$[M_2] =$$

(4.27)

$$\begin{bmatrix} u(x+c)n_y/2 & d_1 & d_2 & d_5 & 0 & -u(x+c)/2 \\ u(x+c)n_z/2 & d_2 & d_3 & d_4 & u(x+c)/2 & 0 \\ u(x-f)n_z/2 & d_2 & d_3 & d_4 & u(x-f)/2 & 0 \\ u(x-a)n_y/2 & d_1 & d_2 & d_5 & 0 & -u(x-a)/2 \\ u(x-a)n_z/2 & d_2 & d_3 & d_4 & u(x-a)/2 & 0 \end{bmatrix}$$

$$[\Psi_2] = [J_y^W \xi(x+c) \quad J_z^W \xi(x+c) \quad J_z^F \xi(x-f) \quad J_y^P \xi(x-a) \quad J_z^P \xi(x-a)]$$

(4.28)

$$\alpha_4 = i n_y / 2 |n_x| , \quad (4.29)$$

and

$$\alpha_5 = -i n_z / 2 |n_x| . \quad (4.30)$$

Following the procedure of Sec. 3, one may derive the expressions for the loop voltage, Poynting vector, impedance and the quality factor Q. The losses on the antenna, the wall as well as on the Faraday shield may be estimated using [J] and surface resistance of the construction materials. Knowing these losses and the Poynting vector into the plasma, the antenna efficiency apart from losses occurring external to the idealized system may be obtained.

## 5. DISCUSSION AND CONCLUSIONS

Following is a summary of the results:

- (i) The exact analytical expressions for the electro-magnetic fields, antenna voltage and impedance have been obtained in-terms-of the antenna current distribution.

(ii) The computational technique for obtaining the self-consistent antenna current distribution has been tested and found to work.

(iii) The role of the Faraday shield has been studied and the concept of the Cross-Fin Antenna which combines the Faraday shield and the antenna in a single composite structure has been introduced.

(iv) In addition, by describing the plasma through its surface impedance we have effectively broken up the boundary value problem into two parts. This procedure would eventually result in computational economy because in the process of optimizing the antenna parameters, one need not recalculate the plasma effects.

REFERENCES

- /1/ EQUIPE TFR, in Plasma Physics and Controlled Nuclear Fusion Research (Proc. 8th Int. Conf., Brussels, 1980) Vol. II, IAEA, Vienna (1981) 75
- /2/ HOSEA, J. et al., Ibid. (1981) 95
- /3/ BHATNAGAR, V.P. et al., Ibid (1981) 85
- /4/ WEYNANTS, R.R., MESSIAEN, A.M., LEBLUD, C., VANDENPLAS, P.E., in Heating in Toroidal Plasmas (Proc. 2nd Grenoble-Varenna Int. Symp. Como, 1980) Vol. I, Brussels (1980) 487
- /5/ BERS, A., JACQUINOT, J., LISTER, G., Ibid (1980) 569
- /6/ MESSIAEN, A.M., WEYNANTS, R.R., BRAL, L., KOCH, R., in Proc. IVth Topical Conference on RF Plasma Heating, Austin (1981) paper A23
- /7/ ADAM, J., JACQUINOT, J., LAPIERRE, Y., MARTY, D., Ibid (1981) paper A1
- /8/ BERS, A., HARTEN, L.P., RAM, A., Ibid (1981) paper A16
- /9/ BHATNAGAR, V.P., KOCH, R., MESSIAEN, A.M., WEYNANTS, R.R., Nuclear Fusion (to be published)

/10/ JORDAN, E.C., BALMAIN, K.G., "Electromagnetic Waves and Radiating Systems", Prentice-Hall Inc., Englewood Cliffs, New Jersey, 1968

/11/ KING, R.W.P., "The Theory of Linear Antennas", Harvard University Press, Cambridge, Massachusetts, 1956.

Fig. 3 Idealized antenna in the dip geometry. The antenna loops possess a width "w" and the adjacent loops are a distance "L" apart along the z-direction.

Fig. 4 Self-consistent current (heavy solid line) for the isolated antenna system with the normalized parameters  $n = 1.0$ ,  $\beta_0 = 1.0$ ,  $\beta_1 = 1.0$ ,  $\beta_2 = 1.0$ ,  $\beta_3 = 1.0$ ,  $\beta_4 = 1.0$ ,  $\beta_5 = 1.0$ ,  $\beta_6 = 1.0$ ,  $\beta_7 = 1.0$ ,  $\beta_8 = 1.0$ ,  $\beta_9 = 1.0$ ,  $\beta_{10} = 1.0$ ,  $\beta_{11} = 1.0$ ,  $\beta_{12} = 1.0$ ,  $\beta_{13} = 1.0$ ,  $\beta_{14} = 1.0$ ,  $\beta_{15} = 1.0$ ,  $\beta_{16} = 1.0$ ,  $\beta_{17} = 1.0$ ,  $\beta_{18} = 1.0$ ,  $\beta_{19} = 1.0$ ,  $\beta_{20} = 1.0$ ,  $\beta_{21} = 1.0$ ,  $\beta_{22} = 1.0$ ,  $\beta_{23} = 1.0$ ,  $\beta_{24} = 1.0$ ,  $\beta_{25} = 1.0$ ,  $\beta_{26} = 1.0$ ,  $\beta_{27} = 1.0$ ,  $\beta_{28} = 1.0$ ,  $\beta_{29} = 1.0$ ,  $\beta_{30} = 1.0$ ,  $\beta_{31} = 1.0$ ,  $\beta_{32} = 1.0$ ,  $\beta_{33} = 1.0$ ,  $\beta_{34} = 1.0$ ,  $\beta_{35} = 1.0$ ,  $\beta_{36} = 1.0$ ,  $\beta_{37} = 1.0$ ,  $\beta_{38} = 1.0$ ,  $\beta_{39} = 1.0$ ,  $\beta_{40} = 1.0$ ,  $\beta_{41} = 1.0$ ,  $\beta_{42} = 1.0$ ,  $\beta_{43} = 1.0$ ,  $\beta_{44} = 1.0$ ,  $\beta_{45} = 1.0$ ,  $\beta_{46} = 1.0$ ,  $\beta_{47} = 1.0$ ,  $\beta_{48} = 1.0$ ,  $\beta_{49} = 1.0$ ,  $\beta_{50} = 1.0$ ,  $\beta_{51} = 1.0$ ,  $\beta_{52} = 1.0$ ,  $\beta_{53} = 1.0$ ,  $\beta_{54} = 1.0$ ,  $\beta_{55} = 1.0$ ,  $\beta_{56} = 1.0$ ,  $\beta_{57} = 1.0$ ,  $\beta_{58} = 1.0$ ,  $\beta_{59} = 1.0$ ,  $\beta_{60} = 1.0$ ,  $\beta_{61} = 1.0$ ,  $\beta_{62} = 1.0$ ,  $\beta_{63} = 1.0$ ,  $\beta_{64} = 1.0$ ,  $\beta_{65} = 1.0$ ,  $\beta_{66} = 1.0$ ,  $\beta_{67} = 1.0$ ,  $\beta_{68} = 1.0$ ,  $\beta_{69} = 1.0$ ,  $\beta_{70} = 1.0$ ,  $\beta_{71} = 1.0$ ,  $\beta_{72} = 1.0$ ,  $\beta_{73} = 1.0$ ,  $\beta_{74} = 1.0$ ,  $\beta_{75} = 1.0$ ,  $\beta_{76} = 1.0$ ,  $\beta_{77} = 1.0$ ,  $\beta_{78} = 1.0$ ,  $\beta_{79} = 1.0$ ,  $\beta_{80} = 1.0$ ,  $\beta_{81} = 1.0$ ,  $\beta_{82} = 1.0$ ,  $\beta_{83} = 1.0$ ,  $\beta_{84} = 1.0$ ,  $\beta_{85} = 1.0$ ,  $\beta_{86} = 1.0$ ,  $\beta_{87} = 1.0$ ,  $\beta_{88} = 1.0$ ,  $\beta_{89} = 1.0$ ,  $\beta_{90} = 1.0$ ,  $\beta_{91} = 1.0$ ,  $\beta_{92} = 1.0$ ,  $\beta_{93} = 1.0$ ,  $\beta_{94} = 1.0$ ,  $\beta_{95} = 1.0$ ,  $\beta_{96} = 1.0$ ,  $\beta_{97} = 1.0$ ,  $\beta_{98} = 1.0$ ,  $\beta_{99} = 1.0$ ,  $\beta_{100} = 1.0$ . The dashed line shows the current variation with free space wavelength variation used as an initial guess in the iterative computational refinement method (3.68a).

Fig. 5 The Cross-Tin Antenna which combines the twin function of wave junction and Faraday shielding in a simple composite structure.

FIGURE CAPTIONS

Fig. 1 Antenna in toroidal geometry

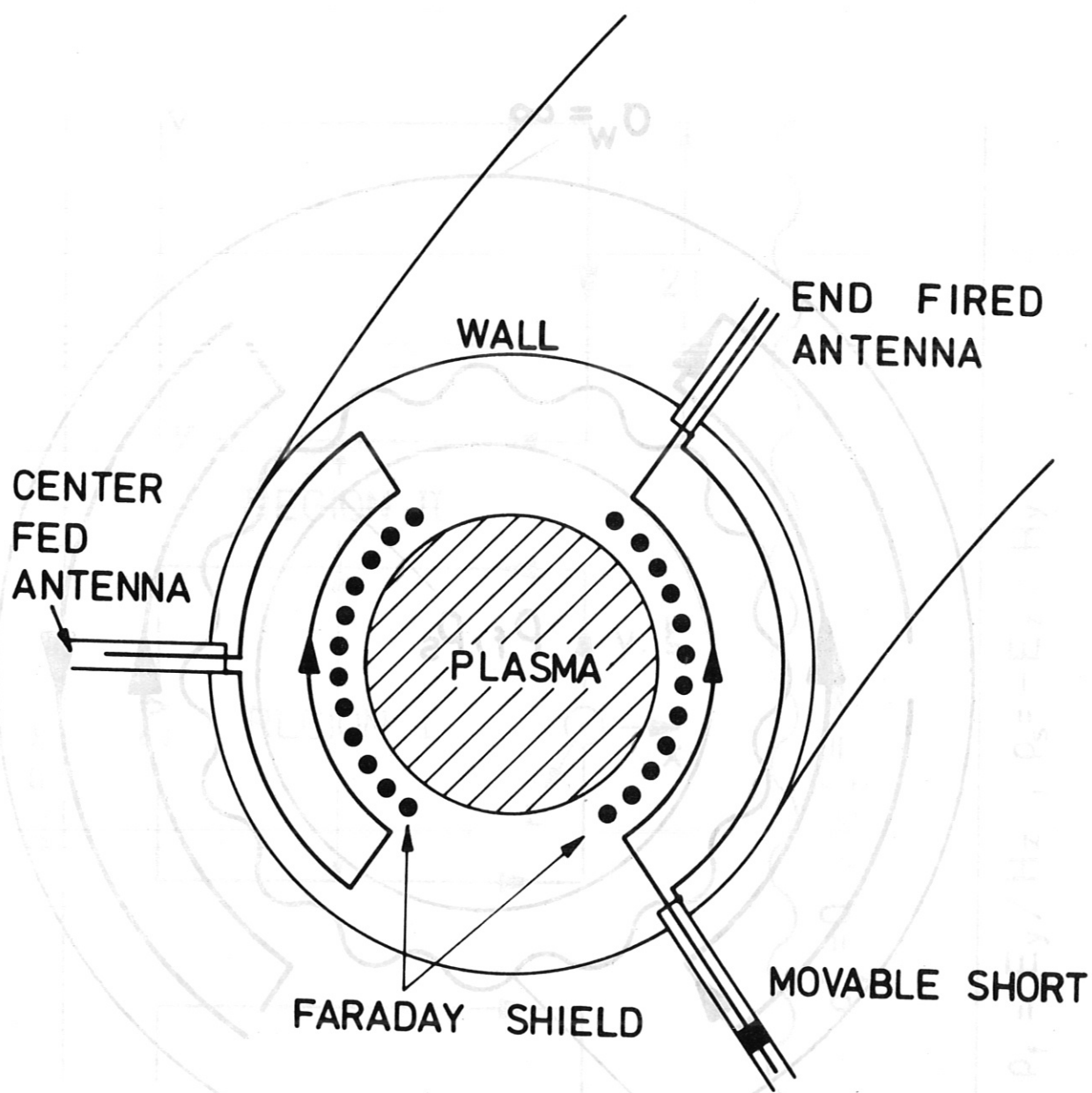
Fig. 2 Idealized antenna in the cylindrical geometry

Fig. 3 Idealized antenna in the slab geometry. The antenna loops possess a width "2w" and the adjacent loops are a distance  $\lambda_{z0}/2$  apart along the z-direction

Fig. 4 Self-consistent current (heavy solid line) for the isolated antenna system with the normalized parameters  $b = 1/32$ ,  $2l = 3/32$ ,  $2v = 1/128$ ,  $2w = 1/16$ ,  $n_{y0} = n_{z0} = 2$ ,  $n_{\xi0} = 1$ . The dashed line shows the current variation with free space wavelength variation used as an initial guess in the iterative computational refinement using (3.68a).

Fig. 5 The Cross-Fin Antenna which combines the twin function of wave launching and Faraday shielding in a single composite structure.





## FIGURE CAPTIONS

Fig. 1 Antenna in toroidal geometry

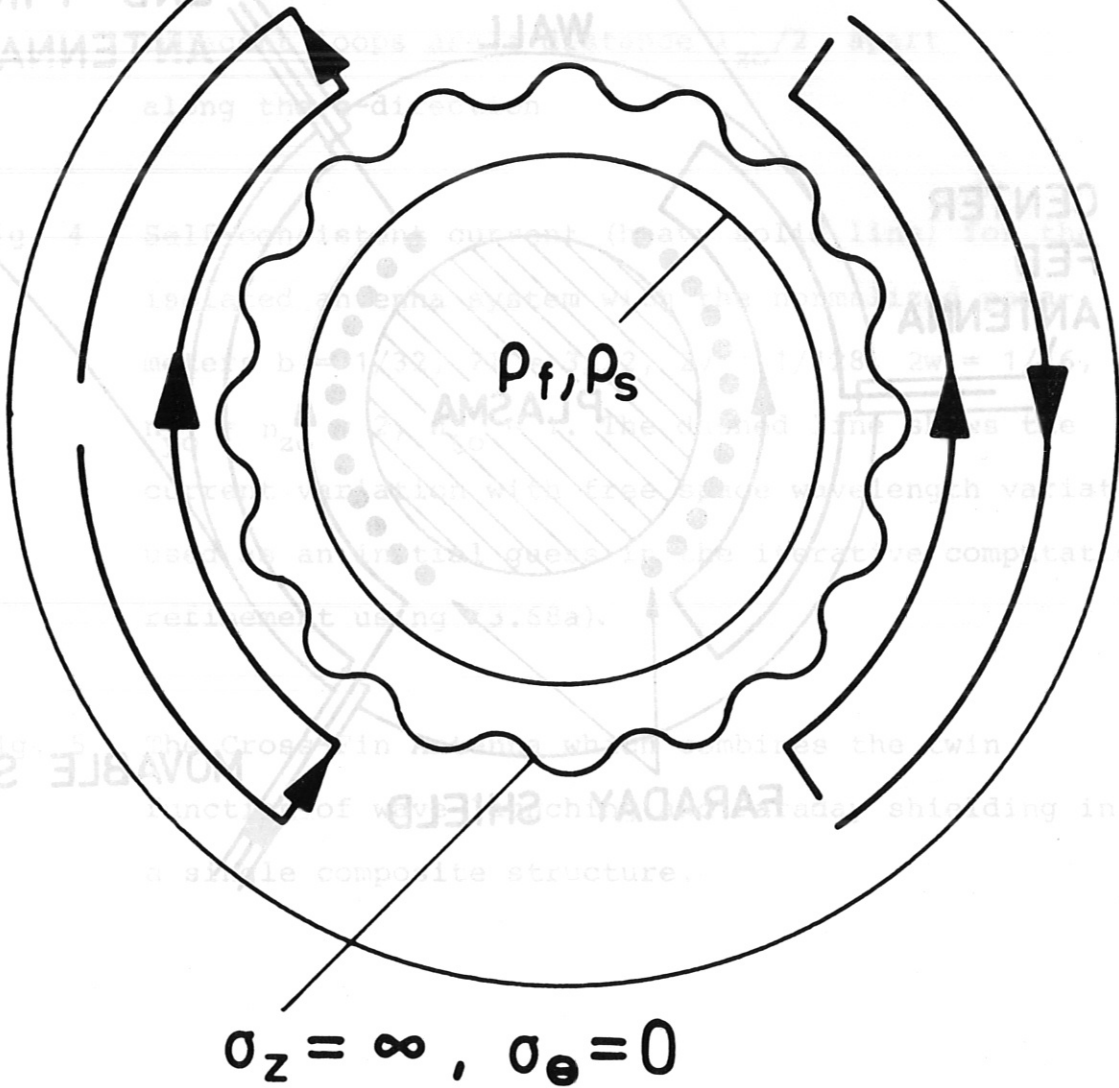
Fig. 2 Idealized antenna in the cylindrical geometry

Fig. 3 Idealized antenna in the slab geometry. The

END FIRED

ANTENNA

ANTENNA



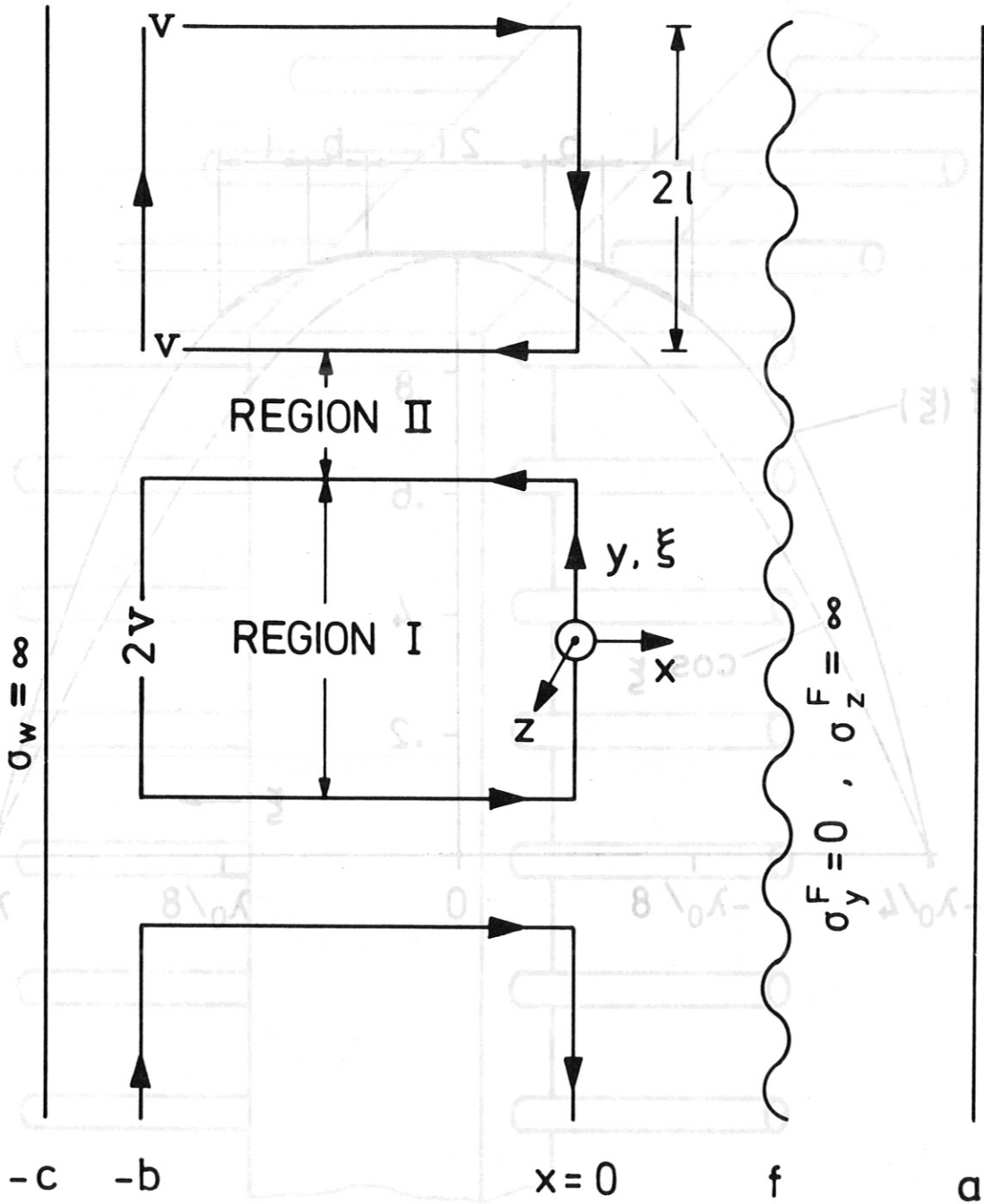
SHORT

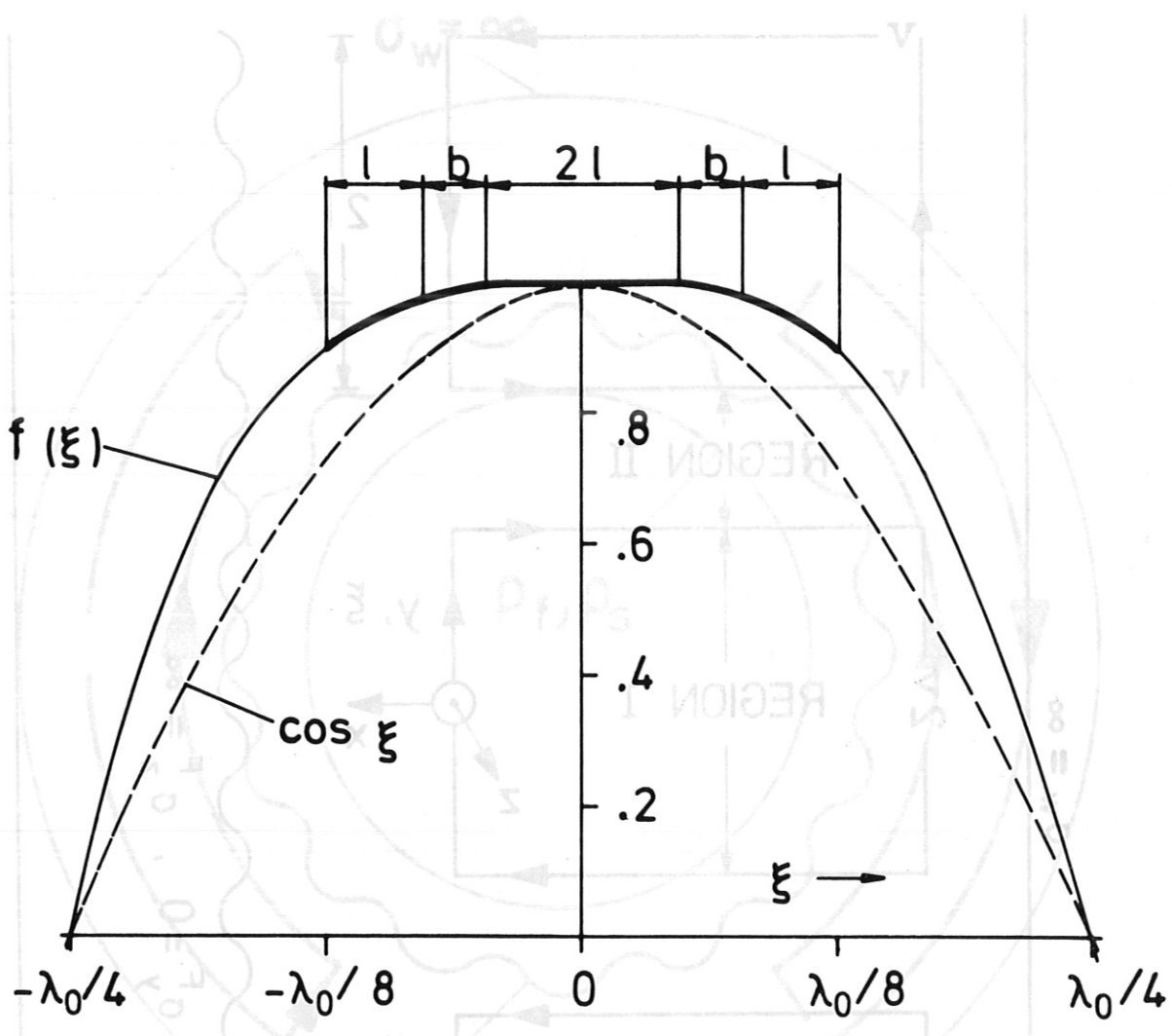
ANTENNA

ANTENNA

ANTENNA

ANTENNA





$$b^2 = E^2 \lambda^2 / H^2 \quad b^2 = -E^2 \lambda^2 / H^2$$

$$\varphi_z = \infty \quad \varphi_x = 0 \quad \varphi_y = 0$$

